Cell

In Vivo Identification of Tumor-Suppressive PTEN ceRNAs in an Oncogenic BRAF-Induced Mouse Model of Melanoma

Florian A. Karreth,[1] Yvonne Tay,[1] Daniele Perna,[3] Ugo Ala,[1,4] Shen Mynn Tan,[5] Alistair G. Rust,[6] Gina DeNicola,[2] Kaitlyn A. Webster,[1] Dror Weiss,[1] Pedro A. Perez-Mancera,[3] Michael Krauthammer,[7] Ruth Halaban,[8] Paolo Provero,[4] David J. Adams,[6] David A. Tuveson,[3] and Pier Paolo Pandolfi[1,*]

[1]Cancer Genetics Program, Division of Genetics

[2]Division of Signal Transduction

Beth Israel Deaconess Cancer Center, Department of Medicine and Pathology, Beth Israel Deaconess Medical Center, Harvard Medical School, Boston, MA 02215, USA

[3]Li-Ka Shing Centre, Cambridge Research Institute, CRUK, Robinson Way, Cambridge CB2 0RE, UK

[4]Molecular Biotechnology Center and Department of Genetics, Biology and Biochemistry, University of Turin, Turin, Italy

[5]Immune Disease Institute and Program in Cellular and Molecular Medicine, Children's Hospital Boston, and Department of Pediatrics, Harvard Medical School, Boston, MA 02115, USA

[6]Experimental Cancer Genetics, Wellcome Trust Sanger Institute, Wellcome Trust Genome Campus, Hinxton, CB10 1HH, UK

[7]Department of Pathology

[8]Department of Dermatology

Yale University, New Haven, CT 06520, USA

*Correspondence: ppandolf@bidmc.harvard.edu

DOI 10.1016/j.cell.2011.09.032

SUMMARY

We recently proposed that competitive endogenous RNAs (ceRNAs) sequester microRNAs to regulate mRNA transcripts containing common microRNA recognition elements (MREs). However, the functional role of ceRNAs in cancer remains unknown. Loss of PTEN, a tumor suppressor regulated by ceRNA activity, frequently occurs in melanoma. Here, we report the discovery of significant enrichment of putative PTEN ceRNAs among genes whose loss accelerates tumorigenesis following Sleeping Beauty insertional mutagenesis in a mouse model of melanoma. We validated several putative PTEN ceRNAs and further characterized one, the *ZEB2* transcript. We show that *ZEB2* modulates PTEN protein levels in a microRNA-dependent, protein coding-independent manner. Attenuation of ZEB2 expression activates the PI3K/AKT pathway, enhances cell transformation, and commonly occurs in human melanomas and other cancers expressing low PTEN levels. Our study genetically identifies multiple putative microRNA decoys for PTEN, validates *ZEB2* mRNA as a bona fide PTEN ceRNA, and demonstrates that abrogated ZEB2 expression cooperates with $BRAF^{V600E}$ to promote melanomagenesis.

INTRODUCTION

Melanoma is estimated to affect more than 70,000 people in the US in the year 2011 and, despite extensive research and clinical efforts, remains fatal in the majority of patients with metastatic disease (http://www.cancer.gov/). Aberrant activation of the MAPK-signaling pathway plays a central role in melanoma development, as exemplified by the frequent occurrence of activating mutations in BRAF (Brose et al., 2002; Davies et al., 2002). Genetic and molecular analyses have demonstrated that oncogenic $BRAF^{V600E}$ represents an initiating event in the evolution of melanoma (Davies et al., 2002). Indeed, 80% of human nevi harbor a $BRAF^{V600E}$ mutation (Pollock et al., 2003). Moreover, mouse models of $BRAF^{V600E}$ develop melanoma only after a long latency and with incomplete penetrance (Dankort et al., 2009; Dhomen et al., 2009; F.A.K., D.P., and D.A.T., unpublished data), suggesting that additional mutations are required for the formation of frank malignancy. Silencing of the tumor suppressor PTEN represents one such mutation and is observed in ~30% of human melanoma cases (Tsao et al., 2004). In mice, complete or partial PTEN loss dramatically accelerates $BRAF^{V600E}$-induced melanoma (Dankort et al., 2009), thus highlighting the oncogenic potential of combined hyperactivation of PI3K/AKT and MAPK signaling.

MicroRNAs (miRNAs) have been shown to regulate PTEN and thus contribute to cell transformation mediated by aberrant activation of the PI3K/AKT pathway (Poliseno et al., 2010a). miRNAs are endogenous, noncoding ~22 nucleotide RNA molecules that bind to microRNA response elements (MREs) contained in their target mRNAs (Bartel, 2009; Thomas et al., 2010). This association recruits the RNA-induced silencing complex (RISC) to target mRNA transcripts, thereby antagonizing their stability and/or translation (Bartel, 2009; Thomas et al., 2010). miRNA-mediated modulation of mRNA levels is conserved in most eukaryotic organisms and is considered a mechanism to fine-tune gene expression. In recent years, numerous examples of abnormal gene regulation by miRNA

misexpression have been demonstrated to contribute to pathological conditions (http://202.38.126.151/hmdd/mirna/md/).

mRNAs harbor multiple MREs and thus can be regulated by several miRNAs, and miRNAs are known to target dozens of mRNA transcripts. The fact that distinct RNA molecules can be targeted by common miRNAs led us to propose that related highly homologous mRNAs, such as gene-pseudogene pairs, may act as miRNA decoys for each other. Pseudogenes are considered "junk DNA," as they lack a protein coding function (D'Errico et al., 2004). However, by binding to common miRNAs, pseudogene mRNAs may maintain the balance between their ancestral genes and such miRNAs. Indeed, we have recently demonstrated that the PTEN pseudogene transcript *PTENP1* regulates the levels of PTEN through sequestration of shared miRNAs (Poliseno et al., 2010b).

On this basis, we further hypothesized that the concept of gene regulation by competition for common miRNAs is not limited to pseudogenes and can be extended to mRNAs and long noncoding RNAs and have termed RNA molecules that act as miRNA decoys as "competitive endogenous RNAs" (ceRNAs) (Salmena et al., 2011). Importantly, we proposed that the mRNA and the protein encoded by ceRNA genes may be involved in distinct biological processes (Salmena et al., 2011). Employing bioinformatics-guided prediction methods of MRE overlap, we have discovered that multiple mRNAs serve as ceRNAs for PTEN (Tay et al., 2011 [this issue of *Cell*]). Importantly, the proteins encoded by PTEN ceRNAs have thus far not been associated with the regulation of PTEN, supporting the notion that, in some instances, mRNAs and the proteins that they encode may be involved in distinct biological processes.

Our recent work suggests that mRNAs may act as tumor suppressors or oncogenes through their ceRNA activity. However, whether aberrant ceRNA expression is associated with cancer development in general and whether loss of PTEN ceRNAs promotes $BRAF^{V600E}$-induced melanoma in vivo in particular are unknown. Here, we report a striking enrichment for PTEN ceRNAs among genes that were identified in a transposon mutagenesis screen in an oncogenic BRAF-driven mouse model of melanoma. Detailed functional analysis of one such putative PTEN ceRNA, *ZEB2*, validated its protein-independent and miRNA-dependent ability to regulate PTEN expression. Moreover, we show that *ZEB2* and *PTEN* are coregulated and that *ZEB2* levels are commonly attenuated in human cancers.

RESULTS

Identification of Putative PTEN ceRNAs Using In Vivo Sleeping Beauty Insertional Mutagenesis

Oncogenic $BRAF^{V600E}$ is an initiating mutation in melanoma, and whereas some other mutations such as loss of PTEN commonly occur in melanoma, the full spectrum of tumor-promoting genetic events remains to be determined. To this end, we performed a forward genetic screen utilizing the Sleeping Beauty transposon system in a $B\text{-}Raf^{V619E}$-driven mouse model of melanoma (Figure S1 and Extended Experimental Procedures available online), in which $B\text{-}Raf^{V619E}$ corresponds to human $BRAF^{V600E}$. A detailed description and in-depth analysis of this screen will be reported elsewhere (F.A.K., D.P., and D.A.T., unpublished data). In brief, we created mutant mice that carried the following alleles: $LoxP\text{-}STOP\text{-}LoxP\text{-}B\text{-}Raf^{V619E}$ (LSL-$B\text{-}Raf^{V619E}$; F.A.K., D.P., and D.A.T., unpublished data), Tyrosinase-CreERt2 (TyrCreERt2 [Bosenberg et al., 2006]), rosa26-LoxP-STOP-LoxP-SleepingBeauty13 (LSL-SB; P.A.P.-M. and D.A.T., unpublished data), and T2Onc (Collier et al., 2005). Treatment of compound mutant LSL-$B\text{-}Raf^{V619E}$; TyrCreERt2; LSL-SB; T2Onc mice with 4-OH Tamoxifen activated the melanocyte-specific Cre, leading to excision of the STOP cassettes and expression of endogenous oncogenic B-Raf and SB13. Sleeping Beauty transposase-mediated "hopping" of the T2Onc transposon resulted in insertional mutagenesis, thereby accelerating melanoma development (Figures 1A and S1 and data not shown). 454 sequencing of genomic melanoma DNA identified 320 genes with a significant enrichment of transposon insertions, termed "common insertion sites" (CIS). Importantly, PTEN was among the most significant CIS (data not shown), thus demonstrating the ability of our Sleeping Beauty mutagenesis approach to identify key genes altered in melanoma.

As loss of PTEN expression cooperates with $BRAF^{V600E}$ (Dankort et al., 2009; Tsao et al., 2004) and PTEN expression is regulated by ceRNAs (Poliseno et al., 2010b; Tay et al., 2011), we sought to determine whether Sleeping Beauty identified putative PTEN ceRNAs that cooperate with $B\text{-}Raf^{V619E}$ to accelerate melanoma development (Figure 1A). We performed a mutually targeted MRE enrichment (MuTaME) analysis (Figure 1B; Tay et al., 2011) using the TargetScan prediction algorithm (Friedman et al., 2009; Grimson et al., 2007; Lewis et al., 2005; http://www.targetscan.org) for MREs located in 3′UTRs. We postulated that the ability of any given mRNA to act as a miRNA decoy for *PTEN* increases with the number of MREs that they share. The 3′UTR of murine *PTEN* was predicted to contain MREs for 39 different miRNAs (Table S1). We set a stringent cutoff of at least seven shared MREs between *PTEN* and putative PTEN ceRNAs for the MuTaME analysis (Figure 1B). Using these conditions, we identified 33 candidate PTEN ceRNAs among the 320 CIS discovered in the Sleeping Beauty screen (Figure 1C). Notably, this represented a significant enrichment of putative PTEN ceRNAs ($p = 7.76 \times 10^{-11}$), as the MRE-based overlap with PTEN expected by chance was only approximately nine genes. Thus, our Sleeping Beauty approach uncovered putative PTEN ceRNAs that promote cancer in an in vivo model of melanoma.

We ranked the 33 putative PTEN ceRNAs according to their similarity with *PTEN* (Figure 2A). The similarity score is based on a Poisson distribution: we used a linear combination, with equal and opposite weights, of the dissimilarity based on distinct occurrences and the additive similarity as defined previously (van Helden, 2004). This approach utilized all miRNAs predicted by TargetScan and the total number of their MREs located in the 3′UTRs to obtain the similarity score for each CIS. Furthermore, most candidate PTEN ceRNAs contain several MREs for the same miRNAs, and thus the total numbers of MREs shared with *PTEN* are even greater (Table S1).

PTEN ceRNAs Modulate Expression of PTEN

To examine whether the identified putative PTEN ceRNAs regulate expression of PTEN, we performed RNAi-mediated gene silencing in human melanoma cells using pools of four siRNAs

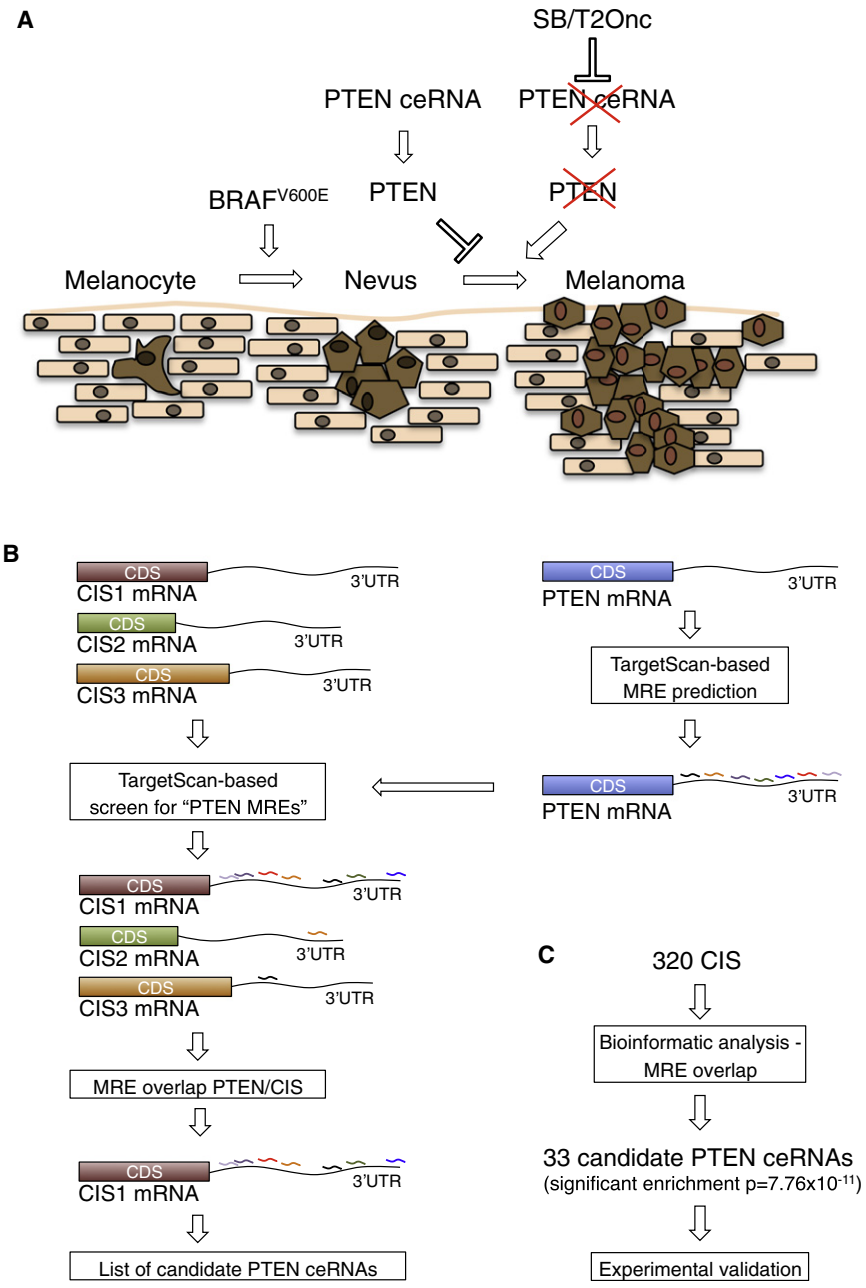

Figure 1. Identification of Putative PTEN ceRNAs

(A) Schematic outline of our hypothesis: oncogenic BRAF mediates the transformation from melanocytes to nevi, and additional loss of PTEN promotes progression to melanoma. PTEN expression is regulated by PTEN ceRNAs, which sequester PTEN-targeting miRNAs. Transposon insertion into ceRNA gene loci suppresses their expression, which results in increased availability of *PTEN*-targeting miRNAs and a reduction of PTEN expression.

(B) Bioinformatics approach to identify putative PTEN ceRNAs among Sleeping Beauty CIS. MREs predicted by TargetScan in the murine *PTEN* 3′UTR were utilized for a mutually targeted MRE enrichment (MuTaME) analysis to determine MRE overlap between *PTEN* and Sleeping Beauty CIS. CIS that share seven or more MREs with *PTEN* were considered putative PTEN ceRNAs.

(C) Enrichment of putative PTEN ceRNAs among Sleeping Beauty CIS. The Sleeping Beauty screen identified 320 CIS, 33 of which are putative PTEN ceRNAs. This enrichment is highly significant ($p = 7.76 \times 10^{-11}$).

See also Table S1 and Figure S1.

to reduce off-target effects. We selected eight putative PTEN ceRNAs (*AFF1*, *DCBLD2*, *JARID2*, *MBNL1*, *RBM9*, *TNRC6a*, *TNRC6b*, and *ZEB2*) and depleted them in WM35 cells (Figure 2B). Knockdown of seven genes led to reduction of PTEN, six of which significantly attenuated PTEN expression (*AFF1*, *JARID2*, *MBNL1*, *RBM9*, *TNRC6a*, *TNRC6b*, and *ZEB2*). A reduction of *PTEN* mRNA levels following PTEN ceRNA silencing was also evident in WM35 cells (Figure S2A). In a second human melanoma cell line, A375, decreased PTEN expression was also observed following PTEN ceRNA knockdown, albeit at lower levels (Figures S2C and S2D). The knockdown efficiencies are shown in Figures S2B and S2E. Interestingly, in some instances, depletion of PTEN resulted in downregulation of the putative PTEN ceRNA (Figures S2B and S2E), indicating that the regulatory relationship between *PTEN* and PTEN ceRNAs might be reciprocal. Importantly, we found that CNOT6L, a PTEN ceRNA that we predicted using the rna22 algorithm and validated in prostate cancer (Tay et al., 2011), was a CIS identified by Sleeping Beauty. Similar to its ceRNA function in prostate cancer cells (Tay et al., 2011), siRNA-mediated knockdown of CNOT6L significantly reduced PTEN expression in both human melanoma cell lines (Figures 2B and S2C).

Critically, the T2Onc transposons inserted in PTEN and the putative PTEN ceRNAs in both orientations throughout the genes (Figure S2F). This insertion pattern is indicative of gene repression via the polyadenylation signals rather than gene activation by the MSCV promoter (Collier et al., 2005). Thus, these CIS are likely tumor suppressors. Taken together, these results indicate that the candidate ceRNAs identified by Sleeping Beauty may indeed act as tumor-suppressive ceRNAs for PTEN.

ZEB2 Silencing Results in Attenuated PTEN Expression

As silencing of several of the putative PTEN ceRNAs led to reduced PTEN protein levels, we sought to further validate and characterize the ability of a CIS mRNA to function as a PTEN ceRNA. None of the seven CIS that reduced PTEN

A

Gene symbol	Similarity score	Common MREs
Pten	1.000	39
Tnrc6b	0.625	27
Zfp148	0.336	16
Taok1	0.287	14
Ubn2	0.280	14
Lrch1	0.253	12
Dcbld2	0.245	12
Cask	0.244	12
Epc2	0.210	10
Bach2	0.209	11
Mll1	0.207	11
Nfia	0.206	11
Tnrc6a	0.197	10
Mbnl1	0.194	10
Epc1	0.192	10
Chd9	0.177	9
Jarid2	0.176	9
Dtna	0.168	9
Zeb2	0.166	9
Aff1	0.158	8
Etv6	0.154	8
Prickle2	0.153	8
Ank3	0.151	8
Rbm9	0.143	8
Rapgef2	0.137	8
Kcna1	0.131	8
Zeb1	0.127	7
Csmd1	0.126	7
Cdk13	0.125	7
Asxl2	0.124	7
Dip2c	0.123	7
Rock2	0.119	7
Slc6a6	0.117	7
Fndc3b	0.111	7

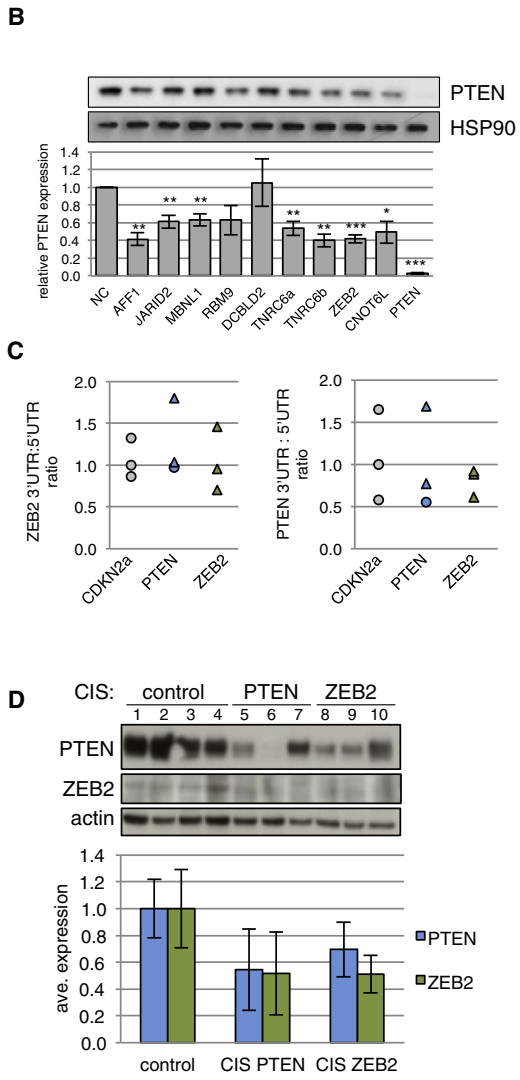

Figure 2. Putative PTEN ceRNAs Modulate PTEN Expression Levels

(A) List of candidate PTEN ceRNAs identified by Sleeping Beauty. The 33 putative PTEN ceRNAs are ranked by their similarity score, which is based on the identity and number of MREs, as well as the length of the CIS 3′UTRs. The number of MREs shared between *PTEN* and the individual CIS is also shown.

(B) Western blot (top) and quantification (bottom) of siRNA-mediated knockdowns of putative PTEN ceRNAs in WM35 human melanoma cells. HSP90 expression is shown as a loading control, and PTEN expression levels were normalized to HSP90.

(C) Transposon insertion does not increase expression of the *ZEB2* 3′UTR (left) or *PTEN* 3′UTR (right). qRT-PCR depicting the ratio between *ZEB2* 5′UTR and 3′UTR expression levels in melanomas with transposon insertions in CDKN2A, PTEN, or ZEB2 is shown.

(D) Melanomas with ZEB2 transposon insertions express less PTEN. Western blot showing expression of PTEN and ZEB2 in melanomas isolated from LSL-B-Raf^{V619E}; TyrCreERt2 mice (control) or LSL-B-Raf^{V619E}; TyrCreERt2; LSL-SB; T2Onc mice with a transposon insertion in either PTEN (CIS: PTEN) or ZEB2 (CIS: ZEB2). Quantification of the western analysis is shown in the bottom panel. Note that PTEN and ZEB2 expression is diminished in tumors with either PTEN or ZEB2 insertions.

NC, negative control (nontargeting siRNA pool). Data are represented as mean ± SEM. See also Figure S2.

levels in WM35 melanoma cells code for a known tumor suppressor protein. The ZEB2 protein, however, has been well established as an activator of the epithelial-to-mesenchymal transition (EMT) (Gregory et al., 2008; Vandewalle et al., 2005) and therefore plays a critical role in the progression of epithelial cancers. Whether the ZEB2 protein is protumorigenic in melanoma is unknown; however, as a PTEN ceRNA, the *ZEB2* mRNA may be tumor suppressive. Given the potentially distinct function of the ZEB2 protein and transcript, we decided to examine whether *ZEB2* mRNA exerts a tumor-suppressive function in melanoma through its competition for PTEN-targeting miRNAs.

Transposon insertions in the 5′-3′ orientation in the ZEB2 locus could theoretically allow for overexpression of the *ZEB2* 3′UTR, which would potentially sequester miRNAs from *PTEN* and result in elevated PTEN levels. To ascertain that the *ZEB2* 3′UTR is not overexpressed in melanomas with such insertions, we analyzed the expression ratio of the *ZEB2* 5′UTR and 3′UTR. Importantly, we observed a 1:1 ratio of expression in all cases, thus excluding overexpression of the 3′UTR (Figure 2C). As an additional control, we tested the effects of transposon insertion in the PTEN locus. Similarly, tumors with transposon insertions in the 5′-3′ orientation did not display an increase in the *PTEN* 3′UTR:5′UTR ratio (Figure 2C), indicating that the transposon acts as a gene trap in these cases. We further tested whether ZEB2 protein levels are affected by transposon insertions. PTEN and ZEB2 are readily detectable by immunoblotting in melanomas without transposon insertions (Figure 2D, lanes 1–4). In contrast, transposon insertion in either PTEN (Figure 2D, lanes 5–7) or ZEB2 (Figure 2D, lanes 8–10) reduced expression of both proteins (Figure 2D). These data confirm that transposon insertion in PTEN and ZEB2 represses gene expression and indicate that ZEB2 reduction modulates protein levels of PTEN. Moreover, the decrease in ZEB2 expression in tumors with a PTEN transposon insertion suggests that the *PTEN-ZEB2* miRNA decoy mechanism may be reciprocal.

To further examine the regulation of PTEN by *ZEB2* via miRNA sequestration, we used pools of four siRNAs to deplete PTEN or ZEB2 in a primary murine melanoma cell line, TB13602, isolated from a LSL-B-Raf^{V619E}; TyrCreERt2 mouse. Knockdown of ZEB2 in TB13602 cells reduced PTEN protein levels by ~60% (Figure 3A). RNAi-mediated silencing of PTEN led to a slight

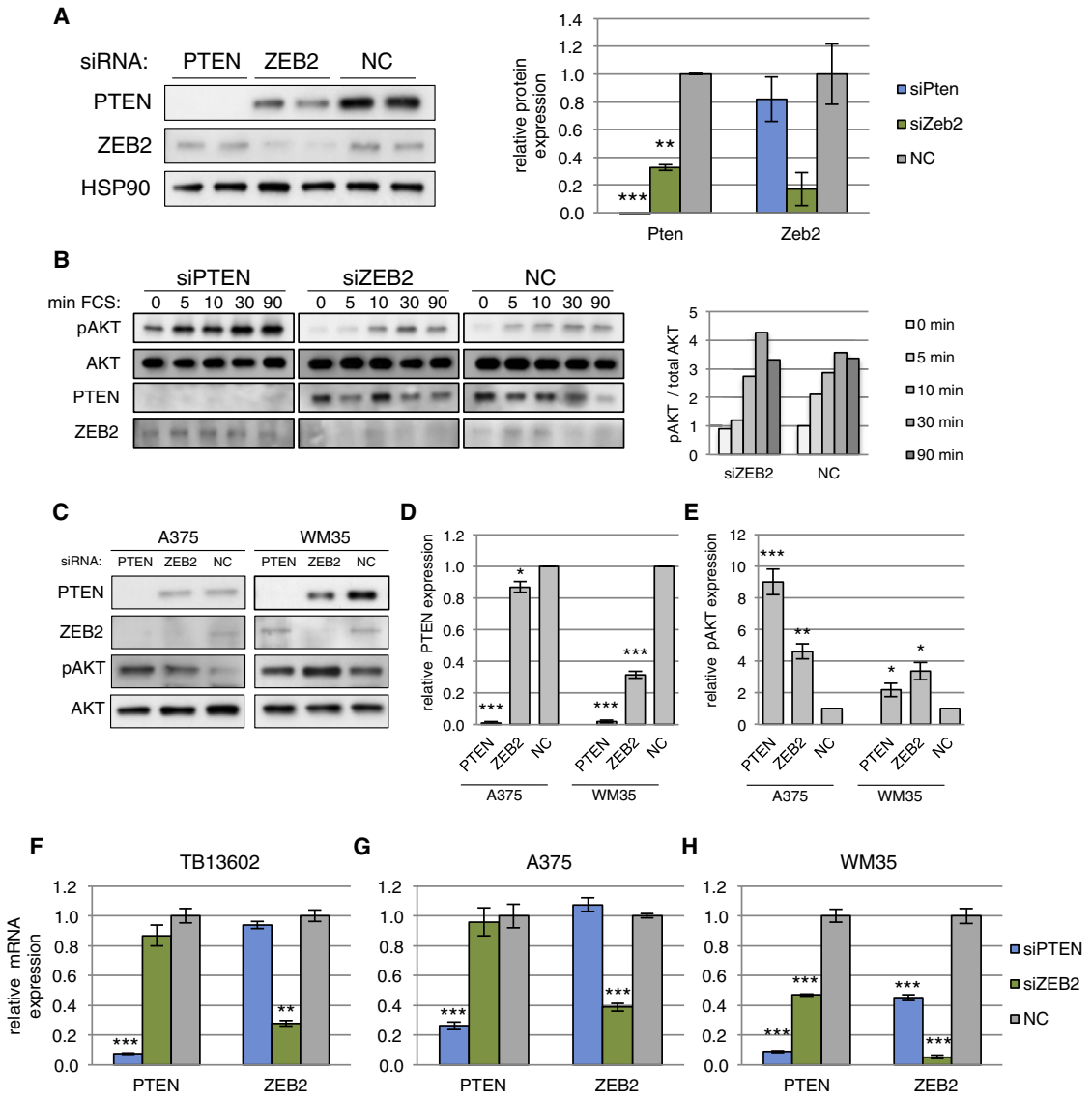

Figure 3. ZEB2 Depletion Downregulates PTEN

(A) ZEB2 silencing lowers PTEN protein levels in murine melanoma cells TB13602. Western analysis for PTEN and ZEB2 expression and HSP90 as loading control is shown in the left panel. Quantification of three independent western analyses is shown in the right panel.

(B) AKT activation kinetics in TB13602 cells following ZEB2 depletion. Cells were starved overnight and stimulated with 10% FCS-containing media for the indicated time points. Western blots for phosphorylated AKT (pAKT), total AKT, ZEB2, and PTEN are shown in the left panel; quantification of pAKT is shown in the right panel.

(C) ZEB2 silencing in human melanoma cell lines lowers PTEN expression and activates AKT. A375 and WM35 melanoma cells lines were transfected with siRNA pools against PTEN or ZEB2. Western analysis for PTEN, ZEB2, and phospho-AKT is shown. HSP90 and total AKT were used as loading controls.

(D) Quantification of PTEN expression in A375 and WM35 cells in three independent western analyses. PTEN expression was normalized to HSP90 levels.

(E) Quantification of AKT activation in A375 and WM35 cells in three independent western analyses. Phospho-AKT expression was normalized to total AKT levels.

(F) qRT-PCR analysis of *PTEN* and *ZEB2* expression in TB13602 cells.

(G and H) qRT-PCR analyses of *PTEN* and *ZEB2* expression in A375 (G) and WM35 (H) cells. Mouse and human siRNA pools against PTEN and ZEB2 efficiently reduce *PTEN* and *ZEB2* mRNA, respectively. Note the reciprocal effect of ZEB2 knockdown on PTEN expression levels and vice versa in WM35 cells.

NC, negative control (nontargeting siRNA pool). Data are represented as mean ± SEM. See also Figure S3.

attenuation of ZEB2 expression (Figure 3A), similar to the results obtained in melanomas with PTEN or ZEB2 CIS (Figure 2D).

As PTEN is a major antagonist of PI3K/AKT signaling, we examined whether *ZEB2*-mediated reduction of PTEN activates this pathway. ZEB2 depletion had no effect on AKT phosphorylation at steady-state levels (data not shown); however, upon starvation and restimulation, ZEB2-depleted cells displayed elevated AKT activation compared to control cells (Figure 3B).

We next analyzed whether *ZEB2* acts as a PTEN ceRNA in human melanoma cells. In four human melanoma cell lines, PTEN protein levels were reduced following knockdown of ZEB2 (Figures 3C, 3D, and S3A). Moreover, depletion of ZEB2 led to AKT activation in these cell lines (Figures 3C, 3E, and S3A). Importantly, ZEB2 siRNAs without potential seed matches to *PTEN* efficiently lowered PTEN levels in mouse and human melanoma cells (Figure S3B), indicating that PTEN downregulation is not due to off-target effects of the ZEB2 siRNA pools. Interestingly, ZEB2 depletion had only minor and statistically insignificant effects on *PTEN* mRNA levels in TB13602 and A375 cells (Figures 3F and 3G), whereas it significantly reduced *PTEN* transcript in WM35 cells (Figure 3H). These data suggest that the miRNAs mediating the functional interaction of *PTEN* and *ZEB2* regulate mRNA stability in a cell line-dependent fashion, whereas their control of translation is a more universal phenomenon.

Repression of PTEN by *ZEB2* Loss Is 3′UTR and miRNA Dependent

These in vitro and in vivo data support the notion that *ZEB2* acts as a PTEN ceRNA. They do not exclude, however, the transcriptional regulation or protein stability as potential mechanisms of *ZEB2* loss-mediated PTEN reduction. We addressed these possibilities by ectopic expression of a luciferase-PTEN3′UTR reporter construct in TB13602 cells, followed by knockdown of PTEN or ZEB2. Silencing of either PTEN or ZEB2 increased the availability of shared miRNAs, thereby suppressing the luciferase-PTEN3′UTR reporter as measured by diminished luciferase activity (Figure 4A). Importantly, as the luciferase-PTEN3′UTR reporter construct is expressed from a CMV promoter and does not code for a PTEN peptide, reduced luciferase activity was dependent on the *PTEN* 3′UTR, thus eliminating transcriptional regulation and protein stability as explanations for the *ZEB2-PTEN* functional interaction.

To exclude the involvement of RNA-binding proteins that could regulate *PTEN* mRNA translation through its 3′UTR, we used cells deficient for the miRNA biogenesis protein Dicer to examine whether *ZEB2* controls PTEN levels in a miRNA-dependent manner. In Dicer wild-type HCT116 colon carcinoma cells, siRNA against ZEB2 lowered PTEN levels, similar to our observation in melanoma cells (Figure 4B). In contrast, ZEB2 depletion failed to reduce PTEN expression in Dicer null HCT116 cells (Figure 4B). Moreover, ZEB2 knockdown decreased *PTEN* mRNA only in Dicer wild-type cells, but not in Dicer-deficient cells (Figure 4C). Conversely, PTEN silencing resulted in diminished *ZEB2* mRNA levels in Dicer wild-type HCT116 cells, which was rescued in Dicer-deficient HCT116 cells (Figure 4C). Similar to PTEN attenuation, AKT activation by ZEB2 silencing is only evident in Dicer wild-type HCT116 cells (Figure 4D). These data indicate that regulation of PTEN expression by *ZEB2* is indeed miRNA dependent.

As ablation of *ZEB2* mRNA reduces PTEN expression due to increased availability of common miRNAs, overexpression of *ZEB2* mRNA should have the opposite effect. However, ectopic expression of full-length *ZEB2* mRNA would also increase ZEB2 protein. We therefore overexpressed only the *ZEB2* 3′UTR to uncouple potential effects of elevated ZEB2 protein on PTEN expression, such as transcriptional regulation, from the miRNA-based regulation via MREs. This approach was also used to show that the 3′UTRs of other putative PTEN ceRNAs increase PTEN levels in prostate cancer (Poliseno et al., 2010b; Tay et al., 2011). We expressed the 3′UTRs of *ZEB2* or *PTEN* in A375 and TB13602 melanoma cells. Cells were cotransfected with the luciferase-PTEN3′UTR reporter construct to measure the ceRNA activity of ectopically expressed 3′UTRs on transcripts containing the *PTEN* 3′UTR. Critically, the *ZEB2* 3′UTR significantly increased the activity of the luciferase-PTEN3′UTR reporter (Figures 4E and 4F). Moreover, PTEN protein levels were increased when the *PTEN* and *ZEB2* 3′UTRs were overexpressed in A375 cells (Figure 4G) and Dicer wild-type HCT116 cells (Figure 4H). Elevated expression of PTEN was rescued by Dicer deficiency in HCT116 cells (Figure 4H). Similarly, overexpression of the *ZEB2* 3′UTR significantly increased the activity of the luciferase-PTEN 3′UTR reporter in HCT116 cells, and Dicer deficiency partially negated this effect. Critically, overexpression of the *ZEB2* coding sequence had no effect on PTEN protein levels in HCT116 cells (Figure S4). Thus, depletion as well as overexpression of *ZEB2* mRNA alters the balance between *PTEN* mRNA and common miRNAs, thereby impacting PTEN expression.

Analysis of miRNAs Common to *PTEN* and *ZEB2*

To elucidate which of the miRNAs predicted to target *PTEN* and *ZEB2* mediate the observed crosstalk, we further characterized the effect of these miRNAs on PTEN and ZEB2 expression. First, we interrogated which MREs were predicted to be common between the 3′UTRs of *PTEN* and *ZEB2*. TargetScan predicted that *PTEN* and *ZEB2* are targets for nine shared miRNA families and that they contain a total of 14 and 16 MREs for these miRNAs, respectively (Figure 5A). Of these miRNAs, several have been validated as *PTEN*-targeting miRNAs (miR-25, miR-32, miR-92ab, miR-141, miR-144, miR-363, and miR-367) (Lee et al., 2010; Poliseno et al., 2010a; Zhang et al., 2010), whereas only the miR-200 family has been validated as repressors of *ZEB2* (Gregory et al., 2008; Korpal et al., 2008; Park et al., 2008). We next delivered miRNA mimics for one member of each miRNA family predicted to target *PTEN* and *ZEB2* to TB13602 cells and analyzed PTEN and ZEB2 protein levels. Of the ten miRNAs tested, four targeted PTEN and ZEB2 to some extent (miR-181, miR-200b, miR-25, and miR-92a) (Figure 5B). We next determined the expression levels of these ten miRNAs in melanoma cells. Interestingly, miRNA expression levels were similar between the three different melanoma cell lines analyzed (Figure 5C), and all four miRNAs that target *PTEN* and *ZEB2* were expressed in the melanoma cell lines (Figure 5C).

Next, we examined whether the four suppressive miRNAs (miR-181, miR-200b, miR-25, and miR-92a) that are expressed in melanoma associate with the 3′UTRs of *PTEN* and *ZEB2*. To this end, we performed RNA immunoprecipitations (RIPs) in melanoma cells using the *PTEN* and *ZEB2* 3′UTRs as baits. Notably, all four miRNAs associated with the 3′UTRs of *PTEN* and *ZEB2*, and a control miRNA with no predicted MRE in *PTEN* and *ZEB2* bound neither 3′UTR (Figure 5D). Furthermore, knockdown of either PTEN or ZEB2 increased miRNA availability, as determined by increased association of miR-92a

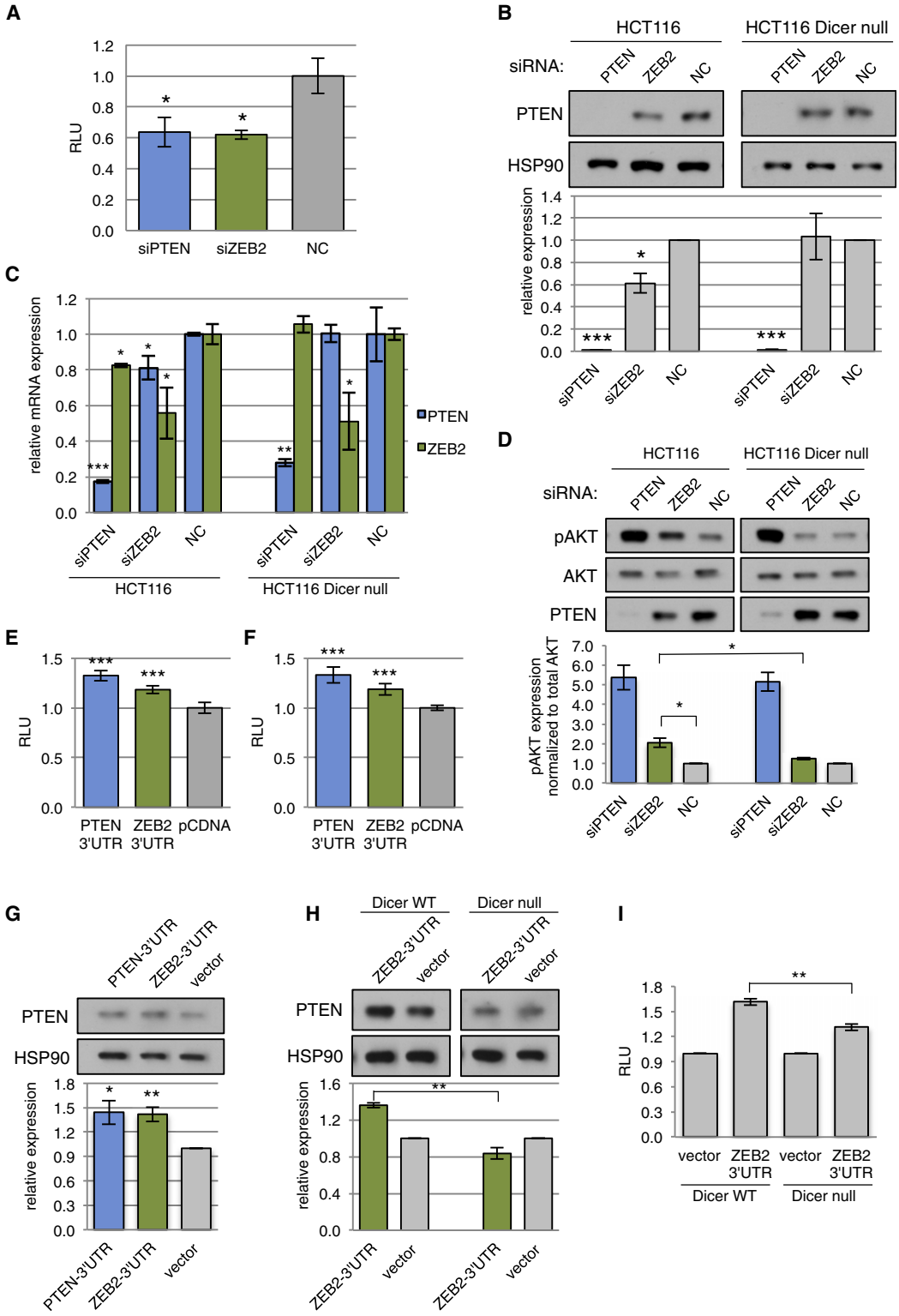

Figure 4. Regulation of PTEN by *ZEB2* Is 3′UTR and miRNA Dependent

(A) Effect of ZEB2 depletion on luciferase activity of a luciferase-PTEN3′UTR reporter. Knockdown of PTEN (positive control) and ZEB2 reduces luciferase activity measured in relative light units (RLU).

(B) ZEB2 depletion lowers PTEN expression in wild-type HCT116 colon cancer cells, but not in Dicer-deficient HCT116 cells. Western blot showing expression of PTEN and HSP90 as loading control in wild-type and Dicer null HCT116 cells (top). (Bottom) Quantification of three independent western blot analyses.

with the MS2-PTEN 3′UTR bait mRNA (Figure 5E). Taken together, *ZEB2* sequesters at least four miRNAs (miR-181, miR-200b, miR-25, and miR-92a) to regulate *PTEN* levels, and *ZEB2* downregulation increases the availability of at least one of these miRNAs.

ZEB2 Displays Tumor-Suppressive Properties in Melanoma Cells

As decreased PTEN expression drives the formation of numerous types of cancer, we determined whether aberrant control of PTEN by loss of *ZEB2* enhanced oncogenic transformation of melanoma cells. Indeed, knockdown of either PTEN or ZEB2 increased proliferation of TB13602 cells (Figure 6A) and WM35 cells (Figure 6B), whereas neither PTEN nor ZEB2 silencing significantly altered the proliferation rate of A375 cells (Figure 6C). Importantly, anchorage-independent growth in soft agar was enhanced by depletion of PTEN or ZEB2 in all three melanoma cell lines (Figures 6D–6F). We next determined whether this ceRNA crosstalk would be operational in vivo. To this end, we lentivirally delivered a short hairpin against ZEB2 to TB13602 cells and examined their oncogenic properties. shRNA-mediated knockdown of ZEB2 lowered expression of PTEN (Figure 6G), accelerated proliferation (Figure 6H), and increased the in vivo growth of xenografted tumors in nude mice (Figure 6I). These data support the notion that ZEB2 has tumor-suppressive activity in melanoma cells, which is, at least in part, due to *ZEB2* mRNA-mediated regulation of PTEN expression.

Functional Crosstalk of *ZEB2* and *PTEN* in Human Cancer

We reasoned that, if *PTEN* and *ZEB2* expression is linked through several shared miRNAs, then their mRNA expression levels might be coregulated. We interrogated mRNA levels in a set of human primary melanoma samples (Halaban et al., 2009) and found that *PTEN* and *ZEB2* expression indeed significantly correlated (Figure 7A). Using the same set of expression data, we asked whether *PTEN* and *ZEB2* expression is diminished in melanomas compared to normal melanocytes. Neither *PTEN* nor *ZEB2* mRNA was significantly decreased in melanomas in this data set (Figure S5A), which is in line with the finding that PTEN expression is lost in only 30% of melanomas (Tsao et al., 2004). We therefore examined whether decreased *ZEB2* expression would be evident in tumors with reduced *PTEN* levels. We subdivided the tumor specimens into two groups: melanomas with *PTEN* expression above average ("PTEN high") and tumors with *PTEN* expression below average ("PTEN low"). Intriguingly, when compared to normal melanocytes, *ZEB2* expression was significantly decreased only in the "PTEN low" subset (Figures 7B and Figure S5A), suggesting that *ZEB2* and *PTEN* mRNAs may coregulate each other in melanoma.

We further determined whether the *PTEN-ZEB2* relationship is specific to melanoma or whether other tumor types display a similar mode of PTEN regulation. Indeed, we identified significant coexpression of *PTEN* and *ZEB2* in primary prostate cancer (Figure 7C). Moreover, *ZEB2* expression is significantly reduced in primary prostate cancer samples with a "PTEN low" expression profile (i.e., PTEN expression level below average) when compared to normal prostatic epithelium or all prostate tumors (Figures 7D and S5B). We analyzed three additional mRNA expression data sets for melanoma, colon carcinoma, and glioblastoma and found that both *PTEN* and *ZEB2* were significantly downregulated in these tumors when compared to normal tissue (Figures 7E–7G). Finally, by interrogating human-mouse conserved and human-specific mRNA coexpression networks, we found that *PTEN* and *ZEB2* mRNA show a significant correlation of coexpression in several human tissues (Figure S5C). Taken together, our data demonstrate that *ZEB2* sequesters miRNAs from *PTEN* and thereby regulates PTEN expression. This mode of PTEN regulation was identified in murine and human melanomas, as well as human prostate, colon, and brain cancer.

DISCUSSION

We report here the identification, functional characterization, and relevance of ceRNAs in cancer biology in vivo. By means of a forward genetics approach using Sleeping Beauty insertional mutagenesis in a mouse model of melanoma, we discovered multiple putative ceRNAs for the tumor suppressor PTEN. Further in vitro characterization validated the EMT regulator ZEB2 as a PTEN ceRNA, and human cancer data corroborated its functional relationship with PTEN. We therefore provide evidence that aberrant regulation of *PTEN* via miRNA competition by ceRNAs contributes to melanoma development.

The results presented here further support our hypothesis that protein-coding mRNAs communicate and coregulate each other through competition for miRNAs that target both transcripts (Salmena et al., 2011; Tay et al., 2011). Importantly, as regulation

(C) *ZEB2* expression is efficiently reduced following treatment of HCT116 cells with ZEB2 siRNA. qRT-PCR analysis of HCT116 cells treated with siRNA for expression of *PTEN* and *ZEB2*.

(D) Activation of AKT following ZEB2 depletion is miRNA dependent. Western blot for pAKT and total AKT in WT and Dicer null HCT116 cells is shown (top). (Bottom) Quantification of three independent western blot analyses.

(E and F) Overexpression of *ZEB* 3′UTR increases *PTEN* 3′UTR reporter activity. A375 (E) or TB13602 (F) melanoma cells were cotransfected with the luciferase-PTEN3′UTR reporter and expression plasmids containing either the *PTEN* 3′UTR or *ZEB2* 3′UTR, followed by luciferase activity measurement 3 days later. The graph depicts the fold increase in RLU when *PTEN* 3′UTR or *ZEB2* 3′UTR was expressed compared to an empty control vector.

(G) Overexpression of *ZEB2* 3′UTR or *PTEN* 3′UTR increases PTEN levels in A375 cells. Western blot for PTEN and HSP90 as a loading control is shown (top). (Bottom) Quantification of PTEN expression in three independent experiments.

(H) Western analyses showing PTEN expression in response to *ZEB2* 3′UTR overexpression in WT and Dicer null HCT116 cells (top). (Bottom) Quantification of three independent western blot analyses.

(I) Effect of overexpression of the *ZEB2* 3′UTR on the activity of a luciferase-PTEN 3′UTR reporter in WT and Dicer null HCT116 cells is shown.

Data are represented as mean ± SEM. NC, negative control (nontargeting siRNA pool). See also Figure S4.

A

Common miRNAs	No. of MREs in Pten	No. of MREs in Zeb2
miR-130/301	3	1
miR-132/212	2	1
miR-141/200a	2	2
miR-144	1	1
miR-153	1	2
miR-181	1	1
miR-200bc/429	1	6
miR-25/32/92/92ab/363/367	1	1
miR-374/374ab	2	1

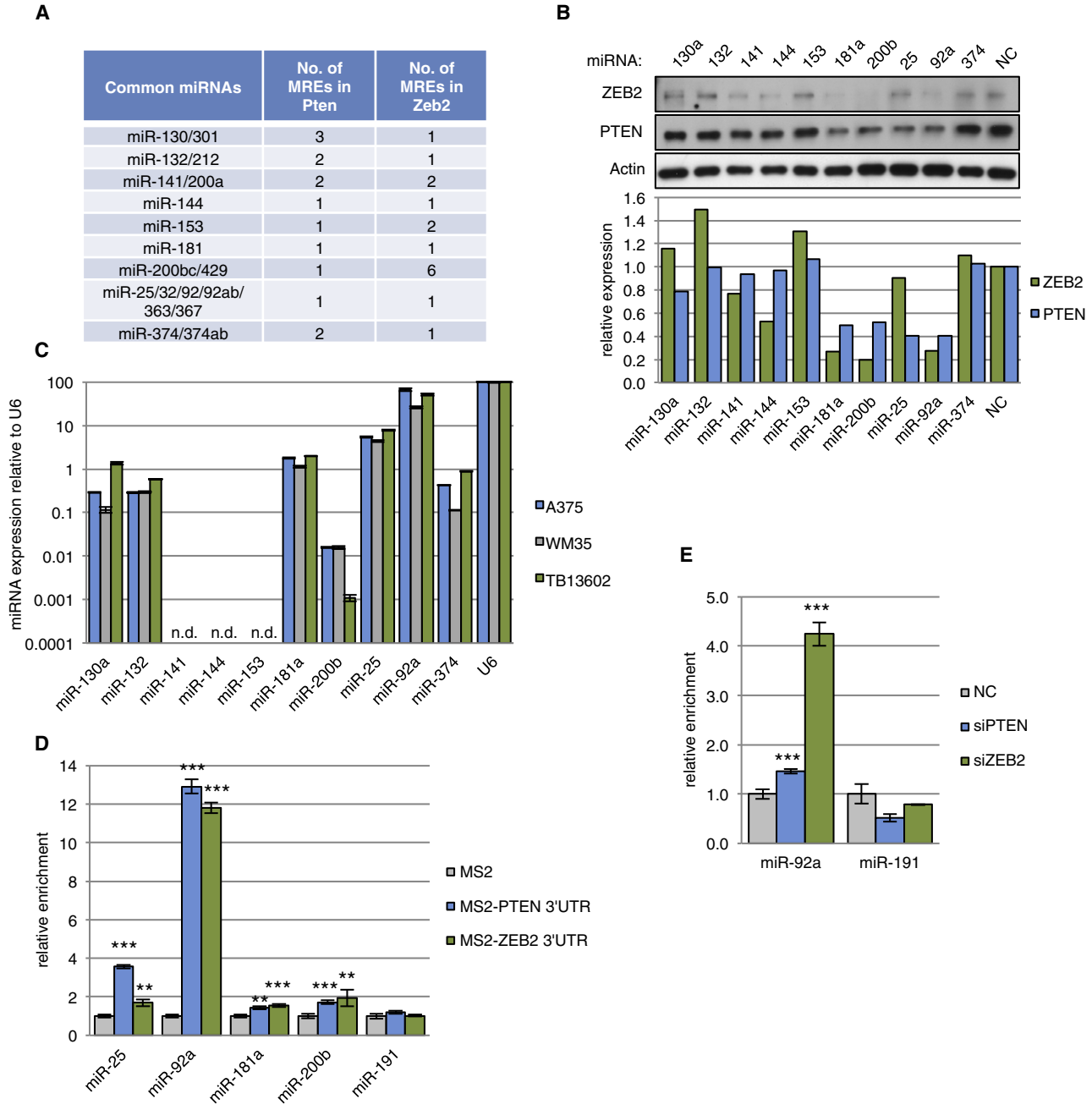

Figure 5. Characterization of miRNAs that Are Common to *PTEN* and *ZEB2*

(A) miRNA response elements (MREs) shared by *PTEN* and *ZEB2*. This table depicts the nine miRNAs that the 3′UTRs of *PTEN* and *ZEB2* have in common, as well as the number of sites for each miRNA.

(B) Multiple miRNAs target both *PTEN* and *ZEB2*. Western analysis of PTEN and ZEB expression in TB13602 melanoma cells treated with the indicated miRNAs is shown. Actin expression is shown as a loading control. Quantification of the western blot is shown in the bottom panel.

(C) Expression of common miRNAs in A375, WM35, and TB13602 melanoma cells as determined by qRT-PCR. n.d., not detectable.

(D) MS2-RIP followed by qRT-PCR to identify endogenous miRNAs associated with the *PTEN* and *ZEB2* 3′UTRs.

(E) MS2-RIP followed by qRT-PCR to identify miRNA binding to the *PTEN* 3′UTR in cells depleted for *PTEN* or *ZEB2*.

NC, negative control (nontargeting siRNA pool). Data are represented as mean ± SEM.

through miRNA sequestration is solely based on MREs, our findings ascribe a predictable and protein coding-independent function to mRNA molecules. Furthermore, we establish a means of regulatory interaction between mRNAs that is based on MREs as functional units. MREs can be found on both protein-coding and noncoding mRNAs, thus challenging the notion that mRNAs are

mere blueprints for peptide synthesis. Though other examples of coding-independent functions of mRNAs have been previously described (Candeias et al., 2008; Jenny et al., 2006), our findings bestow on any RNA molecule functions that may be predicted based on their MRE sequence (Salmena et al., 2011). Our findings of a microRNA-mediated and MRE-dependent gene regulatory ceRNA dimension are corroborated by two other studies demonstrating ceRNA activity for protein coding (Sumazin et al., 2011 [this issue of *Cell*]) and noncoding RNA (Cesana et al., 2011 [this issue of *Cell*]) molecules.

Using bioinformatics approaches and in vitro experimental validation, we have successfully predicted and characterized several ceRNAs that regulate the tumor suppressor PTEN (Tay et al., 2011). In the work presented here, we undertook an unbiased genetic in vivo approach to uncover mutational events that cooperate with oncogenic BRAF to promote melanoma development. Not only did this approach identify PTEN, a known cooperator of oncogenic BRAF in melanoma, but it also generated a list of CIS that was significantly enriched for putative PTEN ceRNAs. Thus, our genetic approach represents an alternative and more functional way of identifying PTEN ceRNAs, which complements our bioinformatics-based ceRNA prediction method.

We have previously used the rna22 prediction algorithm in conjunction with ten validated, 3′UTR-binding *PTEN* miRNAs (miR-17-5p, miR-19a, miR-19b, miR-20a, miR-20b, miR-26a, miR-26b, miR-93, miR-106a, and miR-106b) to predict PTEN ceRNAs (Tay et al., 2011). To screen the murine melanoma CIS for candidate PTEN ceRNAs, we instead employed TargetScan, as this algorithm considers MRE conservation between mammals. TargetScan predicted *PTEN* as a target for 39 different miRNAs (Table S1), which were used to screen the Sleeping Beauty CIS to identify putative PTEN ceRNAs. However, we also compared our list of 320 CIS with the rna22-generated list of putative PTEN ceRNAs and found an overlap of four genes: *CNOT6L*, *MEF2A*, *PDS5B*, and *ROCK2*. These four putative PTEN ceRNAs were not predicted by TargetScan, which is due to the fact that TargetScan considers the miR-17-5p/20ab/93/106ab/519, miR-19ab, and miR-26ab families each as single MREs, whereas we considered them as individual MREs for our rna22-based prediction of PTEN ceRNAs. Thus, though *CNOT6L*, *MEF2A*, *PDS5B*, and *ROCK2* share more than seven MREs with *PTEN* if they are considered individually (rna22 approach), they fall under the threshold of seven MREs if each miRNA family is considered as one MRE (TargetScan approach). Therefore, rna22 and TargetScan prediction algorithms, as well as the use of only validated or all predicted MREs, can successfully be used to predict PTEN ceRNAs. These findings are of great relevance, as they validate and generalize our MuTaME predictions irrespective of the algorithms employed.

We have proposed a set of rules and a methodology to validate and characterize ceRNAs (Tay et al., 2011). By applying this methodology, we have confirmed that *ZEB2* acts as a ceRNA for the tumor suppressor PTEN. Indeed, we found a significant correlation between the expression of *ZEB2* and *PTEN* in human melanomas and prostate cancer (Figure 7). Moreover, compared to benign tissues, *ZEB2* expression was significantly reduced in tumors with low *PTEN* expression levels (Figure 7). Thus, *ZEB2* has tumor-suppressive properties. The ZEB2 protein promotes EMT by repressing expression of E-Cadherin (Vandewalle et al., 2005) and thus may be involved in promoting cancer progression and metastasis in some instances of epithelial cancers. Indeed, the miR-200 family regulates expression of ZEB2 (Gregory et al., 2008; Korpal et al., 2008; Park et al., 2008) and is commonly associated with EMT and cancer progression (Mezzanzanica et al., 2010; O'Day and Lal, 2010; Pang et al., 2010). In melanoma cells, miR-200 does not appear to repress EMT and invasion, but rather, different miR-200 family members mediate alternative modes of melanoma cell migration (Elson-Schwab et al., 2010). It has been reported that ZEB2 expression is suppressed by p53-mediated upregulation of miR-200 (Kim et al., 2011), suggesting that p53 deficiency promotes EMT through induction of ZEB2. However, p53 mutations are rare in melanoma (http://www.sanger.ac.uk/genetics/CGP/cosmic/), making upregulation of ZEB2 via this route unlikely. Moreover, whether EMT is involved in progression of cancers of nonepithelial origin, such as melanoma, is unclear. We hypothesized that, in certain instances, mRNA and protein encoded by the same gene may exert different biological effects (Salmena et al., 2011). ZEB2 powerfully exemplifies such a case, acting as a tumor suppressor by regulating PTEN expression through its mRNA in melanoma, whereas the protein promotes tumor progression and metastasis by controlling EMT in epithelial cancers.

Insertional mutagenesis screens using retroviruses or transposons have been widely used to discover cancer genes. Our work encourages the integration of the classic "protein dimension" with an additional "ceRNA dimension" when analyzing the "hits" of such screens. By doing so, genes that are initially classified as false positives based on their protein function may, in fact, be cancer-promoting genes by means of their ceRNA activity. In addition, previously performed insertional mutagenesis screens could be re-interrogated for the presence of ceRNAs of prominent cancer genes using bioinformatics MRE prediction methods described here and in Tay et al. (2011). This may reveal a so far unappreciated genetic dimension, with a role in cancer development and the pathogenesis of other human conditions.

EXPERIMENTAL PROCEDURES

Plasmids

The 3′UTRs of mouse and human *ZEB2* and human *PTEN* were amplified by PCR from genomic DNA and cloned into pCDNA3 or pCMV according to standard procedures. Generation of PTEN3′UTR-psiCHECK-2 is described by Tay et al. (2011). Primer sequences are available upon request.

Cell Culture and Transfection

A375, WM35, 451Lu, and WM278 human melanoma cells were obtained from M. Herlyn (Wistar Institute) and cultured as previously reported (Tsao et al., 2004). TB13602, HCT116 wild-type, and *Dicer*$^{-/-}$ cells were grown in Dulbecco's modified Eagle's medium (DMEM) supplemented with 10% FCS, penicillin/streptomycin, and glutamine at 37°C in a humidified atmosphere with 5% CO2. Cells were transfected with 100 nM siRNAs and Dharmafect 1 or 1.5 ug of plasmid DNA and Lipofectamine 2000 in 12-well plates according to the manufacturer's recommendations for transfection.

Western Blot Analysis

Cells were lysed in RIPA buffer containing Complete Mini protease inhibitors (Roche) and a Phosphatase Inhibitor cocktail (Sigma). Total protein (5–20 μg)

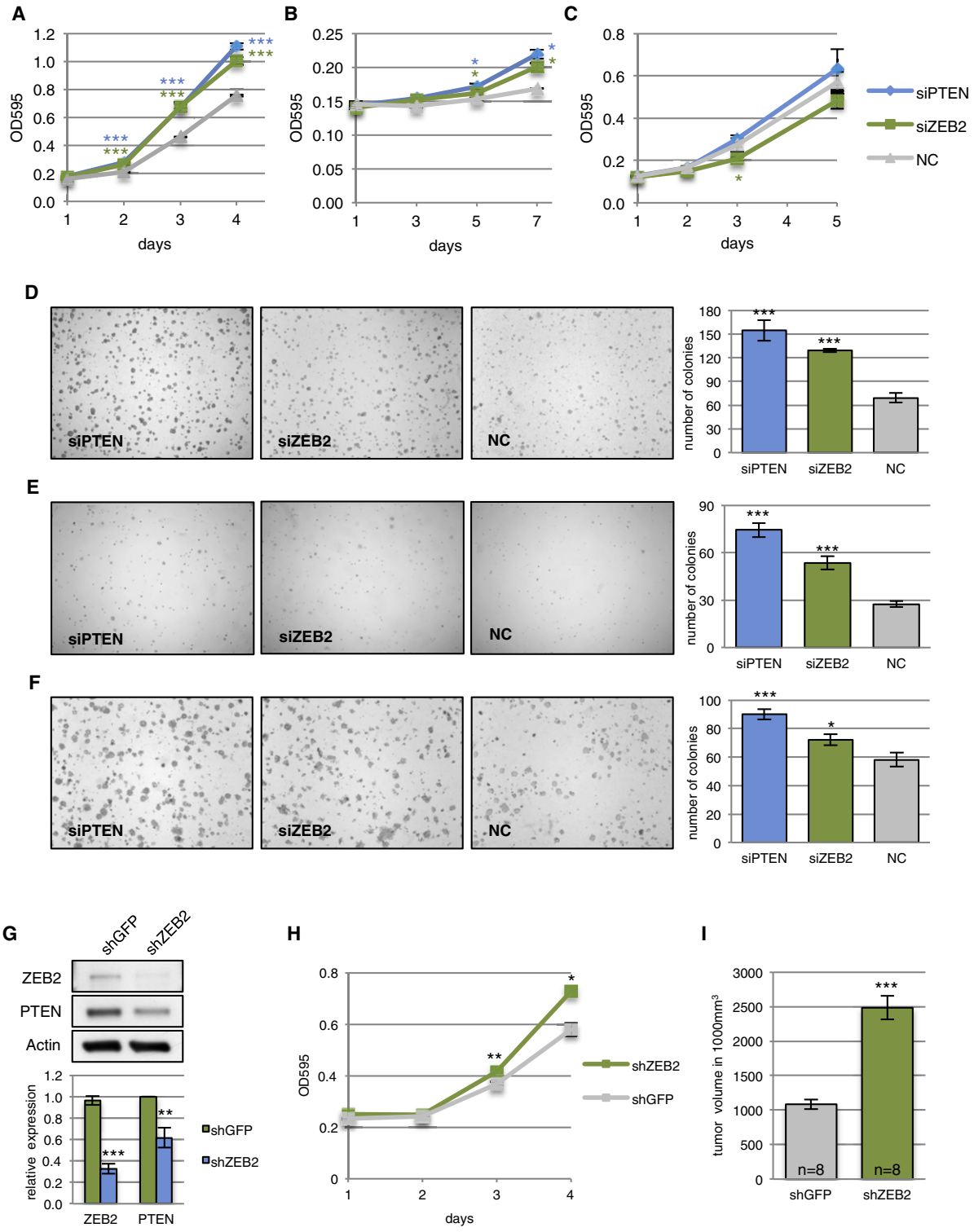

Figure 6. ZEB2 Displays Tumor-Suppressive Properties in Melanoma Cells

(A–C) Proliferation curves of TB13602 (A), WM35 (B), and A375 (C) melanoma cells treated with siPTEN, siZEB2, and NC are shown.

(D–F) Anchorage-independent growth in soft agar. Representative pictures of TB13602 (D), WM35 (E), and A375 (F) are shown on the right, and quantifications are shown on the left.

(G) Western blot showing ZEB2 and PTEN expression in TB13602 cells infected with shZEB2 and shGFP pLKO.1 lentiviruses (top). (Bottom) Quantification of western analysis.

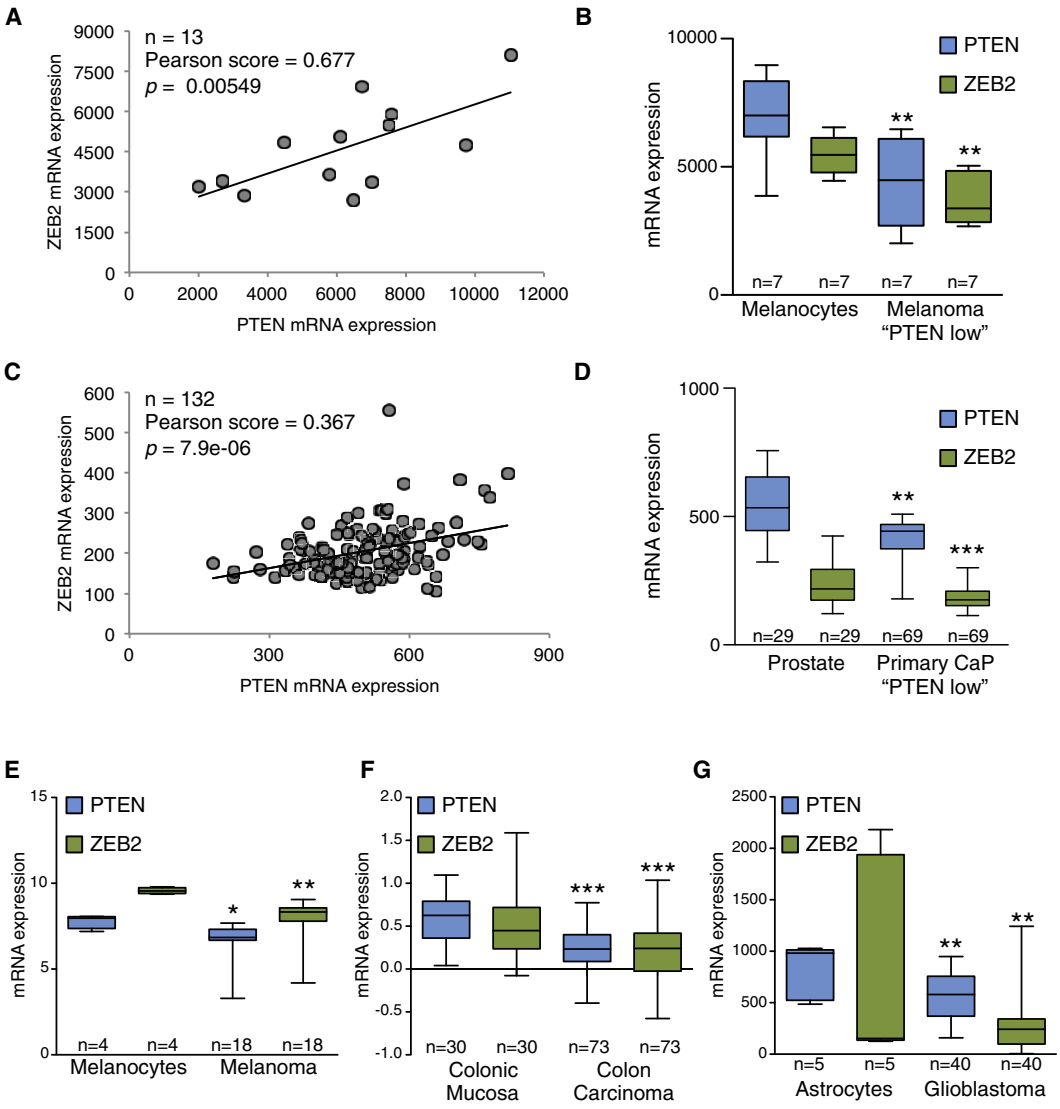

Figure 7. Functional Crosstalk of *PTEN* and *ZEB2* in Human Cancer

(A) mRNA expression of *PTEN* and *ZEB2* correlates in human melanoma. Graph showing mRNA expression levels for *PTEN* and *ZEB2* in human melanoma samples, in which each dot corresponds to one tumor sample. Pearson score shows a positive and significant correlation.

(B) *ZEB2* mRNA expression is significantly lower in human melanomas with reduced *PTEN* expression when compared to normal melanocytes. Box plot depicting mRNA expression levels for *PTEN* and *ZEB2* in normal melanocytes and "PTEN low" tumors (melanomas with *PTEN* mRNA expression below the average).

(C) Correlation of *PTEN* and *ZEB2* mRNA expression in human prostate cancer samples. Similar to (A), each dot represents one tumor sample. Pearson score shows a positive and significant correlation.

(D) *ZEB2* expression is significantly reduced in prostate tumors with low *PTEN* mRNA expression levels. Box plot showing *PTEN* and *ZEB2* mRNA expression levels in normal adjacent prostate and primary prostate adenocarcinoma.

(E–G) Additional mRNA expression data sets showing reduced *PTEN* and *ZEB2* mRNA levels in melanoma (E), colon carcinoma (F), and glioblastoma (G) compared to normal tissue.

In the box plots, the top and bottom boxes represent the 75th and 25th percentile, respectively, and the whiskers represent the minimum and maximum of all data points. See also Figure S5.

was subjected to SDS-PAGE on 4%–12% Bis-Tris acrylamide NuPAGE gels in MOPS SDS buffer (Invitrogen). The following primary antibodies were used: HSP90 (BD), PTEN, phospho-AKT (p473), and total-AKT (Cell Signaling) and ZEB2 and actin (Santa Cruz Biotechnologies). Subsequently, membranes were incubated with secondary HRP-tagged antibodies (Amersham), and signals were visualized with ECL or ECL plus (Amersham).

(H) Proliferation curves of cells shown in (G).

(I) Quantification of xenograft tumor volume of TB13602 cells infected with shZEB2 and shGFP pLKO.1 lentiviruses.

Data are represented as mean ± SEM. NC, negative control (nontargeting siRNA pool).

RNA Extraction and Real-Time PCR

For real-time PCR analyses, total RNA was extracted using the Qiashredders and RNeasy Mini Kit (QIAGEN) according to the manufacturer's recommendations. cDNA was synthesized using the High Capacity cDNA Reverse Transcriptase Kit according to the manufacturer's instructions (Applied Biosystems) and was analyzed by real-time PCR using taqman gene expression assays (Applied Biosystems) on a LightCycler 480 System (Roche Applied Science).

Luciferase Assays

TB13602 or A375 cells were transfected with 150 ng of empty psiCHECK2 vector or psiCHECK2-PTEN3′UTR and either 100 nM siRNA or 1 μg 3′UTR vector constructs using Lipofectamine 2000 according to manufacturer's recommendations. In all transfections, firefly luciferase activity was used as a normalization control for transfection efficiency. Seventy-two hours after transfection, luciferase activities were measured consecutively with the dual luciferase reporter system (Promega) using a luminometer (Promega).

Cell Proliferation

Cells were plated in triplicates in 12-well plates at a final density of 2×10^4/well. On days 1–4 after plating, cells were washed with PBS, fixed in 4% PFA, and stained with crystal violet. The dye was extracted with 10% acetic acid, and absorbance at 595 nm was determined.

Xenografts

1×10^6 TB13602 cells were mixed with Matrigel and injected into the flanks of NCR nude mice. Tumor growth was measured after 14 days and the volume calculated using the formula $0.5 \times L \times W \times H$.

Statistical Analysis

In vitro data were analyzed using unpaired Student's t test. Values of $p < 0.05$ were considered statistically significant. *$p < 0.05$; **$p < 0.01$; ***$p < 0.001$. The mean ± SE of three or more independent experiments performed in triplicates is reported.

SUPPLEMENTAL INFORMATION

Supplemental Information includes Extended Experimental Procedures, five figures, and one table and can be found with this article online at doi:10.1016/j.cell.2011.09.032.

ACKNOWLEDGMENTS

We thank Pandolfi and Tuveson laboratory members for critical discussions. qRT-PCR analysis was conducted with support from Harvard Catalyst | The Harvard Clinical and Translational Science Center (NIH award #UL1 RR 025758 and financial contributions from Harvard University and its affiliated academic health care centers). The content is solely the responsibility of the authors and does not necessarily represent the official views of Harvard Catalyst, Harvard University and its affiliated academic health care centers, the National Center for Research Resources, or the National Institutes of Health. We thank B. Vogelstein for *DICER*$^{-/-}$ cells and M. Bosenberg for TyrCreERt2 mice. We thank F. Connor and other members of the Tuveson lab for assistance and the animal care staff and histology core at CRI. Mice were maintained in compliance with the UK home office regulations. This research was supported by the University of Cambridge, Cancer Research UK, The Li Ka Shing Foundation, Hutchison Whampoa Limited, the NIHR Cambridge Biomedical Research Centre, and The Wellcome Trust. Y.T. was supported by a Special Fellow Award from The Leukemia & Lymphoma Society. D.P. received an International Fellowship in Cancer Research from the Italian Association for Cancer Research (AIRC). P.A.P.-M. was supported by the Fundación Ibercaja. U.A. received a fellowship from the Fondazione per la Ricerca Biomedica ONLUS of Torino. S.M.T. was supported by a Department of Defense Breast Cancer Research Program fellowship. P.P. and U.A. received support from AIRC under grant IG-9408. This work was supported by the Yale SPORE in Skin Cancer funded by the National Cancer Institute grant number 1 P50 CA121974 to R.H. and by NIH grant R01 CA-82328-09 to P.P.P.

Received: August 12, 2011
Revised: September 20, 2011
Accepted: September 24, 2011
Published: October 13, 2011

REFERENCES

Bartel, D.P. (2009). MicroRNAs: target recognition and regulatory functions. Cell *136*, 215–233.

Bosenberg, M., Muthusamy, V., Curley, D.P., Wang, Z., Hobbs, C., Nelson, B., Nogueira, C., Horner, J.W., II, Depinho, R., and Chin, L. (2006). Characterization of melanocyte-specific inducible Cre recombinase transgenic mice. Genesis *44*, 262–267.

Brose, M.S., Volpe, P., Feldman, M., Kumar, M., Rishi, I., Gerrero, R., Einhorn, E., Herlyn, M., Minna, J., Nicholson, A., et al. (2002). BRAF and RAS mutations in human lung cancer and melanoma. Cancer Res. *62*, 6997–7000.

Candeias, M.M., Malbert-Colas, L., Powell, D.J., Daskalogianni, C., Maslon, M.M., Naski, N., Bourougaa, K., Calvo, F., and Fåhraeus, R. (2008). P53 mRNA controls p53 activity by managing Mdm2 functions. Nat. Cell Biol. *10*, 1098–1105.

Cesana, M., Cacchiarelli, D., Legnini, I., Santini, T., Sthandier, O., Chinappi, M., Tramontano, A., and Bozzoni, I. (2011). A long noncoding RNA controls muscle differentiation by functioning as a competing endogenous RNA. Cell *147*, this issue, 358–369.

Collier, L.S., Carlson, C.M., Ravimohan, S., Dupuy, A.J., and Largaespada, D.A. (2005). Cancer gene discovery in solid tumours using transposon-based somatic mutagenesis in the mouse. Nature *436*, 272–276.

D'Errico, I., Gadaleta, G., and Saccone, C. (2004). Pseudogenes in metazoa: origin and features. Brief. Funct. Genomics Proteomics *3*, 157–167.

Dankort, D., Curley, D.P., Cartlidge, R.A., Nelson, B., Karnezis, A.N., Damsky, W.E., Jr., You, M.J., DePinho, R.A., McMahon, M., and Bosenberg, M. (2009). Braf(V600E) cooperates with Pten loss to induce metastatic melanoma. Nat. Genet. *41*, 544–552.

Davies, H., Bignell, G.R., Cox, C., Stephens, P., Edkins, S., Clegg, S., Teague, J., Woffendin, H., Garnett, M.J., Bottomley, W., et al. (2002). Mutations of the BRAF gene in human cancer. Nature *417*, 949–954.

Dhomen, N., Reis-Filho, J.S., da Rocha Dias, S., Hayward, R., Savage, K., Delmas, V., Larue, L., Pritchard, C., and Marais, R. (2009). Oncogenic Braf induces melanocyte senescence and melanoma in mice. Cancer Cell *15*, 294–303.

Elson-Schwab, I., Lorentzen, A., and Marshall, C.J. (2010). MicroRNA-200 family members differentially regulate morphological plasticity and mode of melanoma cell invasion. PLoS ONE *5*, e13176.

Friedman, R.C., Farh, K.K., Burge, C.B., and Bartel, D.P. (2009). Most mammalian mRNAs are conserved targets of microRNAs. Genome Res. *19*, 92–105.

Gregory, P.A., Bert, A.G., Paterson, E.L., Barry, S.C., Tsykin, A., Farshid, G., Vadas, M.A., Khew-Goodall, Y., and Goodall, G.J. (2008). The miR-200 family and miR-205 regulate epithelial to mesenchymal transition by targeting ZEB1 and SIP1. Nat. Cell Biol. *10*, 593–601.

Grimson, A., Farh, K.K., Johnston, W.K., Garrett-Engele, P., Lim, L.P., and Bartel, D.P. (2007). MicroRNA targeting specificity in mammals: determinants beyond seed pairing. Mol. Cell *27*, 91–105.

Halaban, R., Krauthammer, M., Pelizzola, M., Cheng, E., Kovacs, D., Sznol, M., Ariyan, S., Narayan, D., Bacchiocchi, A., Molinaro, A., et al. (2009). Integrative analysis of epigenetic modulation in melanoma cell response to decitabine: clinical implications. PLoS ONE *4*, e4563.

Jenny, A., Hachet, O., Závorszky, P., Cyrklaff, A., Weston, M.D., Johnston, D.S., Erdélyi, M., and Ephrussi, A. (2006). A translation-independent role of oskar RNA in early Drosophila oogenesis. Development *133*, 2827–2833.

Kim, T., Veronese, A., Pichiorri, F., Lee, T.J., Jeon, Y.J., Volinia, S., Pineau, P., Marchio, A., Palatini, J., Suh, S.S., et al. (2011). p53 regulates epithelial-mesenchymal transition through microRNAs targeting ZEB1 and ZEB2. J. Exp. Med. *208*, 875–883.

Korpal, M., Lee, E.S., Hu, G., and Kang, Y. (2008). The miR-200 family inhibits epithelial-mesenchymal transition and cancer cell migration by direct targeting of E-cadherin transcriptional repressors ZEB1 and ZEB2. J. Biol. Chem. *283*, 14910–14914.

Lee, D.Y., Jeyapalan, Z., Fang, L., Yang, J., Zhang, Y., Yee, A.Y., Li, M., Du, W.W., Shatseva, T., and Yang, B.B. (2010). Expression of versican 3′-untranslated region modulates endogenous microRNA functions. PLoS ONE *5*, e13599.

Lewis, B.P., Burge, C.B., and Bartel, D.P. (2005). Conserved seed pairing, often flanked by adenosines, indicates that thousands of human genes are microRNA targets. Cell *120*, 15–20.

Mezzanzanica, D., Bagnoli, M., De Cecco, L., Valeri, B., and Canevari, S. (2010). Role of microRNAs in ovarian cancer pathogenesis and potential clinical implications. Int. J. Biochem. Cell Biol. *42*, 1262–1272.

O'Day, E., and Lal, A. (2010). MicroRNAs and their target gene networks in breast cancer. Breast Cancer Res. *12*, 201.

Pang, Y., Young, C.Y., and Yuan, H. (2010). MicroRNAs and prostate cancer. Acta Biochim. Biophys. Sin. (Shanghai) *42*, 363–369.

Park, S.M., Gaur, A.B., Lengyel, E., and Peter, M.E. (2008). The miR-200 family determines the epithelial phenotype of cancer cells by targeting the E-cadherin repressors ZEB1 and ZEB2. Genes Dev. *22*, 894–907.

Piro, R.M., Ala, U., Molineris, I., Grassi, E., Bracco, C., Perego, G.P., Provero, P., and Di Cunto, F. (2011). An atlas of tissue-specific conserved coexpression for functional annotation and disease gene prediction. Eur. J. Hum. Genet. Published online June 8, 2011. 10.1038/ejhg.2011.96.

Poliseno, L., Salmena, L., Riccardi, L., Fornari, A., Song, M.S., Hobbs, R.M., Sportoletti, P., Varmeh, S., Egia, A., Fedele, G., et al. (2010a). Identification of the miR-106b∼25 microRNA cluster as a proto-oncogenic PTEN-targeting intron that cooperates with its host gene MCM7 in transformation. Sci. Signal. *3*, ra29.

Poliseno, L., Salmena, L., Zhang, J., Carver, B., Haveman, W.J., and Pandolfi, P.P. (2010b). A coding-independent function of gene and pseudogene mRNAs regulates tumour biology. Nature *465*, 1033–1038.

Pollock, P.M., Harper, U.L., Hansen, K.S., Yudt, L.M., Stark, M., Robbins, C.M., Moses, T.Y., Hostetter, G., Wagner, U., Kakareka, J., et al. (2003). High frequency of BRAF mutations in nevi. Nat. Genet. *33*, 19–20.

Salmena, L., Poliseno, L., Tay, Y., Kats, L., and Pandolfi, P.P. (2011). A ceRNA hypothesis: the Rosetta Stone of a hidden RNA language? Cell *146*, 353–358.

Sumazin, P., Yang, X., Chiu, H.-S., Chung, W.-J., Iyer, A., Llobet-Navas, D., Rajbhandari, P., Bansal, M., Guarnieri, P., Silva, J., et al. (2011). An extensive microRNA-mediated network of RNA-RNA interactions regulates established oncogenic pathways in glioblastoma. Cell *147*, this issue, 370–381.

Tay, Y., Kats, L., Salmena, L., Weiss, D., Tan, S.M., Ala, U., Karreth, F., Poliseno, L., Provero, P., Di Cunto, F., et al. (2011). Coding-independent regulation of the tumor suppressor PTEN by competing endogenous mRNAs. Cell *147*, this issue, 344–357.

Thomas, M., Lieberman, J., and Lal, A. (2010). Desperately seeking microRNA targets. Nat. Struct. Mol. Biol. *17*, 1169–1174.

Tsao, H., Goel, V., Wu, H., Yang, G., and Haluska, F.G. (2004). Genetic interaction between NRAS and BRAF mutations and PTEN/MMAC1 inactivation in melanoma. J. Invest. Dermatol. *122*, 337–341.

van Helden, J. (2004). Metrics for comparing regulatory sequences on the basis of pattern counts. Bioinformatics *20*, 399–406.

Vandewalle, C., Comijn, J., De Craene, B., Vermassen, P., Bruyneel, E., Andersen, H., Tulchinsky, E., Van Roy, F., and Berx, G. (2005). SIP1/ZEB2 induces EMT by repressing genes of different epithelial cell-cell junctions. Nucleic Acids Res. *33*, 6566–6578.

Zhang, L., Deng, T., Li, X., Liu, H., Zhou, H., Ma, J., Wu, M., Zhou, M., Shen, S., Li, X., et al. (2010). microRNA-141 is involved in a nasopharyngeal carcinoma-related genes network. Carcinogenesis *31*, 559–566.